
[View Journal Online](#)  
[View Article Online](#)

# Effect of calcination temperature on the structure and morphology of zinc oxide nanoparticles synthesized by base-catalyzed aqueous sol-gel process

Samreen Zahra <sup>1,\*</sup>, Saboora Qaisar <sup>2</sup>, Asma Sheikh <sup>3</sup>,  
 Hamim Bukhari <sup>2</sup>, and Chaudhry Athar Amin <sup>1</sup>

<sup>1</sup> Mineral Processing Research Centre, Pakistan Council of Scientific and Industrial Research Laboratories Complex, Ferozpur Road, Lahore-54600, Pakistan

<sup>2</sup> Department of Chemistry, Post Graduate Islamia College, Cooper Road, Lahore-54000, Pakistan

<sup>3</sup> Biotechnology and Food Research Centre, Pakistan Council of Scientific and Industrial Research Laboratories Complex, Ferozpur Road, Lahore-54600, Pakistan

\* Corresponding author at: Mineral Processing Research Centre, Pakistan Council of Scientific and Industrial Research Laboratories Complex, Ferozpur Road, Lahore-54600, Pakistan.

e-mail: [samreenzahra68@hotmail.com](mailto:samreenzahra68@hotmail.com) (S. Zahra).

## RESEARCH ARTICLE



doi 10.5155/eurjchem.13.2.162-167.2231

Received: 22 February 2022

Received in revised form: 07 April 2022

Accepted: 22 April 2022

Published online: 30 June 2022

Printed: 30 June 2022

## KEYWORDS

Zinc oxide  
 Calcination  
 Nanoparticles  
 Base catalyzed  
 Sol-gel process  
 Crystal structure

## ABSTRACT

This study reports the base-catalyzed aqueous sol-gel synthesis of zinc oxide nanoparticles. The solution was primarily comprised of zinc nitrate hexahydrate as a metal precursor, isopropyl alcohol and water as solvents, and glycerin as a stabilizing agent. The effect of calcination temperature on the structure and morphology of the prepared nanoparticles was investigated by varying the calcination temperature from 500 to 900 °C. The X-ray diffraction analysis, infrared spectroscopy, thermogravimetric analysis, and field emission scanning electron microscopy were employed to determine the crystal structure, surface functional groups, thermal stability, and surface morphology of the nanoparticles. The particle size was found to be directly proportional to the calcination temperature.

Cite this: *Eur. J. Chem.* 2022, 13(2), 162-167

Journal website: [www.eurjchem.com](http://www.eurjchem.com)

## 1. Introduction

Published reports revealed that metal and metal oxide nanoparticles have received remarkable attention owing to their wide range of applications in fields like medicine, electronics, sensors, catalysis, and waste treatment process. Nanosize oxides of metals like iron, zinc, copper, nickel, cobalt, manganese, etc. have been reported for their enhanced physical properties including fine particle size, improved thermal stability, increased surface area, high catalytic activity, and easy usage. Among these metal oxides, zinc oxide is categorized as a semiconductor with a broad band gap energy of 3.37 eV and high bond energy of 60 meV that make it a right choice for use in electronics, optoelectronics, laser technology, sensors, converters, energy generators, photocatalysts, ceramics, bio-medicines and pro-ecological systems [1]. Zinc oxide nanoparticles have an advantage of being versatile in the capability of attaining a variety of structures compared to other metal oxide nanoparticles i.e. they can be produced in one-, two-, and three-dimensional structures including nanorods, needles, helices, springs, and rings, ribbons, tubes, belts, wires and

combs, nanoplates, nano-pellets, flowers, dandelion, snow-flakes, etc. The desired morphology can be obtained by varying synthesis parameters such as reaction temperature, reaction time, agitation speed, the solvent used, pH, calcination temperature, calcination time, etc. [1,2].

Various physical and chemical methods such as sol-gel, precipitation, coprecipitation, colloidal method, hydrothermal, solvothermal, sonochemical and microemulsion, pyrolysis, and inert gas condensation methods have been adopted to produce zinc oxide nanoparticles [3]. Nowadays, researchers are paying more attention to simple, inexpensive, nontoxic, and environment friendly methods for the synthesis of zinc oxide nano-structures [4-6]. Among these methods, the sol-gel technique has been found to be the most appropriate one, being simple, economical, and capable of producing ultrafine materials with high surface area [7]. This method is capable of producing high-quality homogenous and porous structures including nanoparticles, thin-films, xerogels, aerogels, fibres, etc. at low processing temperature [8]. Moreover, it offers the use of a wide range of reagents suitable for controlling the morphology

of nanoparticles. All these facts make sol-gel synthesis being advantageous over green synthesis.

Previous scientists have therefore successfully prepared zinc oxide nanostructures with controlled morphology and size using the most convenient and trouble-free sol-gel technique. Lu *et al.* synthesized three-dimensionally interconnected macropores of zinc oxide using citric acid and an epoxide through sol-gel process together with phase separation [9]. Recently, Vishwakarma and co-workers successfully synthesized ultrafine zinc oxide particles ranging from 15 nm to 25 nm in size [10]. More recently, Somoghi *et al.* reported the base-catalyzed sol-gel preparation of zinc oxide nanoparticles controlled with various silane coupling agents (Octyltriethoxysilane, octadecyltriethoxysilane, and (3-glycidioxypropyl) trimethoxysilane) [11].

Present work deals with the preparation of zinc oxide nanoparticles via a sol-gel process in a basic medium, utilizing zinc nitrate hexahydrate, isopropyl alcohol, and water as a precursor and solvents respectively whereas glycerin was employed as a stabilizing agent. The morphology and structure of the prepared samples were ascertained although X-ray diffraction as well as field emission scanning electron microscopy. Thermal stability was confirmed by thermogravimetry while the presence of surface functional groups was checked by infrared spectroscopy.

## 2. Experimental

### 2.1. Materials

Analytical grade zinc nitrate hexahydrate, isopropyl alcohol, glycerin, and ammonium hydroxide were used for the whole experimental work.

### 2.2. Sample preparation

Zinc oxide nanoparticles were synthesized through an aqueous sol-gel route in a basic medium. Zinc nitrate hexahydrate precursor (14.64 g) was added to a mixture of solvents, i.e. isopropyl alcohol and water in a 1:5 ratio. 8 mL of glycerin were added and the pH of the aqueous solution was maintained at 8 using ammonium hydroxide. The mixture was stirred constantly for two hours at 70 °C. The resulting precipitates were filtered and were dried at 70 °C for several hours until complete drying. The dried precipitates were ground well and were divided into five portions that were calcined for two hours at 500, 600, 700, 800, and 900 °C and were labeled as ZNB-1, ZNB-2, ZNB-3, ZNB-4, and ZNB-5, respectively.

### 2.3. Characterization

X-ray diffraction analysis of all the prepared zinc oxide nanoparticles was carried out by Bruker D2-Phaser X-ray diffractometer employing monochromatized CuK $\alpha$ 1 radiation at a wavelength of 1.54060 Å. Thermal analysis was performed using a Leco TGA701 Thermogravimetric analyzer varying the temperature from room temperature to 1000 °C. IR spectra were recorded with Thermo Nicolet IR 200 (USA) and surface morphology was studied by field emission scanning electron microscope FEI Nova 450 NanoSEM.

## 3. Results and discussion

Synthesis of zinc oxide nanoparticles was carried out in a basic medium using a mixture of isopropanol and water as solvent. Glycerin was added for making polyol medium which acts as both solvent as well as a stabilizing agent for regulating the growth of zinc oxide nanoparticles. The polyol medium is believed to control the formation of hard agglomerates formed

during the synthesis of metal oxide nanoparticles obtained through aqueous routes, therefore the use of high boiling polyols has been recommended by previous researchers [12]. Moreover, the presence of a basic medium in sol-gel synthesis leads to the formation of more hydroxyl groups, thereby facilitating a rapid accomplishment of equilibrium between hydrolysis and condensation reactions [13]. Hence zinc nitrate used as a precursor can readily undergo hydrolysis forming nitrate ions and zinc ions making zinc ions easily available for bonding with the hydroxyl groups of alcohol molecules. The intermediate product, i.e., zinc hydroxide nitrate thus formed in the aqueous solution can be easily transformed into zinc oxide through calcination at higher temperatures. Ammonium nitrate formed as a byproduct is highly soluble in water and can be easily removed. High purity zinc oxide nanoparticles can therefore be obtained successfully by the base-catalyzed aqueous sol-gel route.

### 3.1. X-ray diffraction analysis

Figures 1a-e present the crystal structure of ZNB samples calcined at 500, 600, 700, 800, and 900 °C, respectively. At 500 °C, the pattern shows several diffraction peaks that correspond to the hexagonal wurtzite phase of zinc oxide. Two major peaks for ZNB-1 appear at 31.73 and 36.18° 2 $\theta$  values while minor peaks at 34.36, 47.36, 56.41, 62.33, and 68.64° confirming the presence of the wurtzite phase can be seen (JCPDS Card no: 36-1451). These results are in close agreement with the observations of previous scientists [14-17].

The figures illustrate similar diffraction peaks with slight variation in intensities with the increasing calcination temperature. This can be attributed to the fact that while annealing at higher temperatures the grain growth of nanoparticles occurs resulting in the appearance of more intense and prominent major peaks. The sharpness of the peaks specifies that the samples are well crystallized [18]. However, the broadening of peaks observed at lower calcination temperatures proves the formation of nanosize crystals [19]. Narrowness in diffraction peaks at higher calcination temperatures occurs due to variation in the water of crystallization in molecules of precursor, resulting in more shrinkage subject to the particle coarsening effect due to calcination [20]. Among all the ZNB samples no diffraction peak for any other phase of zinc oxide can be seen, that indicates high purity of single-phase zinc oxide nanoparticles [16]. According to Lu *et al.* pure wurtzite phase of zinc oxide, ZnO could be obtained at calcination temperatures above 320 °C, with simultaneous isotropic shrinkages [9].

### 3.2. Infrared spectroscopy

The IR spectra of zinc oxide nanoparticles prepared in a basic medium recorded in the frequency range of 4000-400 cm<sup>-1</sup> are demonstrated in Figures 2a-e. The figures show similar absorption bands with slight variation in intensity among all samples. Numerous distinct absorption bands were detected in the region between 3800-3000 cm<sup>-1</sup> that are assigned to the stretching modes of hydroxyl groups of water molecules adsorbed on the surface as well as hydrogen-bonded hydroxyl groups [21,22].

The bands of relatively low intensity between 3000-2800 cm<sup>-1</sup> are attributed to the stretching vibrations of alkyl groups of organic impurities captured by the crystals of zinc oxide during their synthesis [11,23,24]. A few weak absorption bands in the region between 2800 and 2200 cm<sup>-1</sup> correspond to hydrogen bonding between surface adsorbed water molecules. Minor absorption bands around 1600 cm<sup>-1</sup> are assigned to the bending vibrations of hydroxyl groups of water molecules [25-27]. Another minor absorption band between 1400 to 1300 cm<sup>-1</sup> can be related to the asymmetric stretching vibrations of the nitrate group [28].

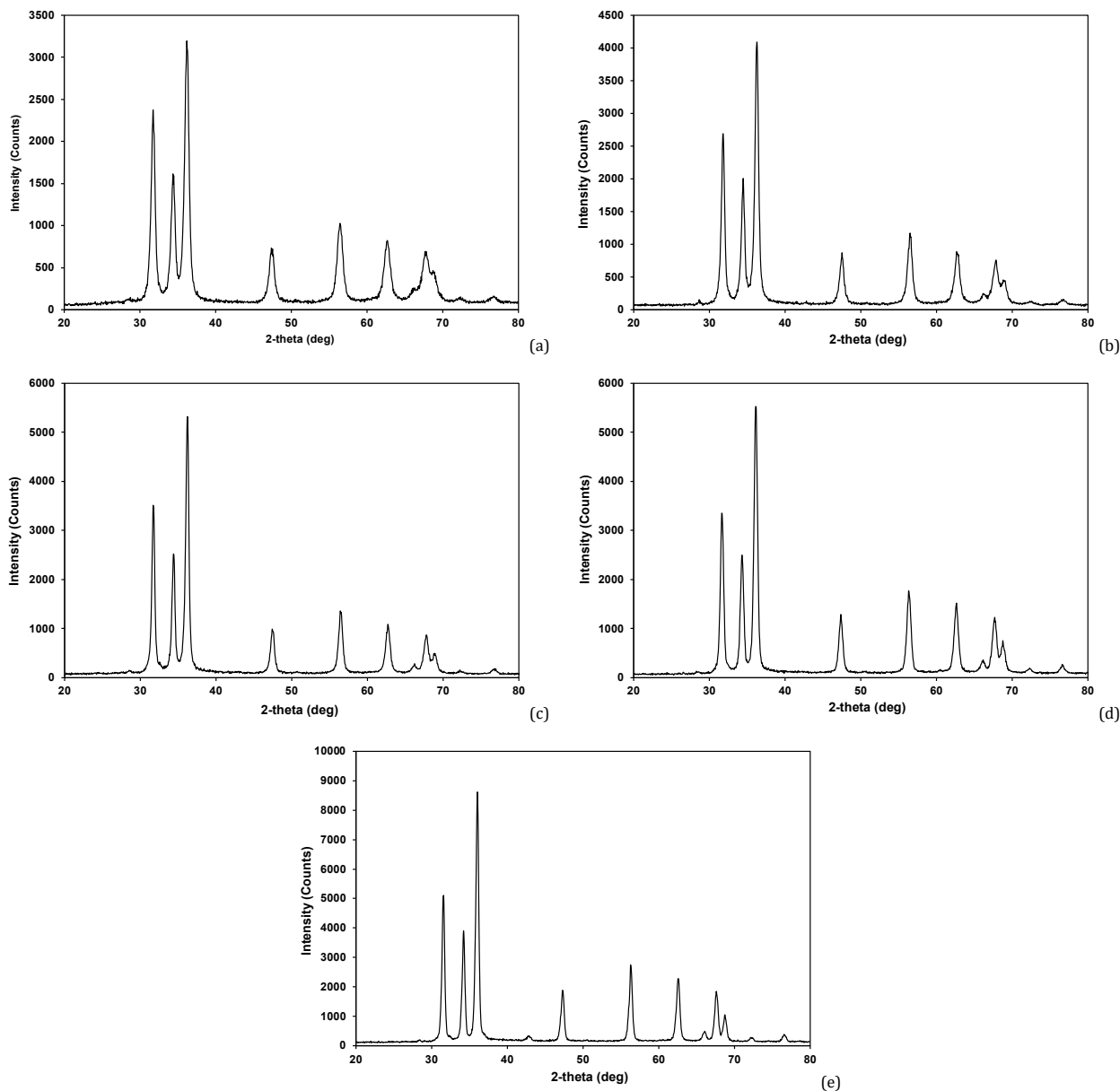


Figure 1. X-ray diffraction pattern of (a) ZNB-1, (b) ZNB-2, (c) ZNB-3, (d) ZNB-4 and (e) ZNB-5.

The prominent broad band below  $1000\text{ cm}^{-1}$  obtained in each ZNB sample except ZNB-2 having an absorption band with relatively low intensity corresponds to the stretching vibrations of metal-oxygen bonds hence proving the formation of Zn-O bonds of zinc oxide. Previous researchers also had similar observations for zinc oxide nanoparticles [7,29].

### 3.3. Thermal analysis

Thermogravimetric analysis of ZNB samples was performed and the curves are shown in Figures 3a-e. The curves show two step gradual weight loss up to  $1000\text{ }^{\circ}\text{C}$ . In the first step below  $400\text{ }^{\circ}\text{C}$ , weight loss of 0.41 to 0.90% observed can be ascribed to the evaporation of adsorbed moisture and organic residues entangled in the mesopores formed between the crystallites during their agglomeration [30,31]. The second step of weight loss of 0.65 to 1.46% till  $1000\text{ }^{\circ}\text{C}$  may take place due to the flow of heat between the sample and the crucible. Hence, these results prove the thermal stability of ZNB samples since no major weight loss occurred among all samples.

### 3.4. Field emission scanning electron microscopy

The surface morphology of the synthesized zinc oxide nanoparticles ZNB-1, ZNB-3, and ZNB-5 was studied by field emission scanning electron microscopy. The images were recorded at  $100,000\times$  magnification and are presented in Figures 4a-c, respectively. The micrograph of ZNB-1 calcined at  $500\text{ }^{\circ}\text{C}$  exhibits agglomerated morphology with nanoparticles of various shapes and multiple sizes gathered to form aggregates in several nanometer ranges. According to previous researchers, chemical binding of primarily formed fine particles results in the formation of aggregates that join to form larger agglomerates through van der Waals forces [32]. However, it can be seen that with the rise in calcination temperature, the agglomeration significantly decreases whereas the size of nanoparticles increases due to particle growth at higher calcination temperatures resulting in the formation of flakes [33]. Hence, ZNB-5 bears a flake-like morphology with a bigger size of flakes and less agglomeration, unlike ZNB-1 and ZNB-3.

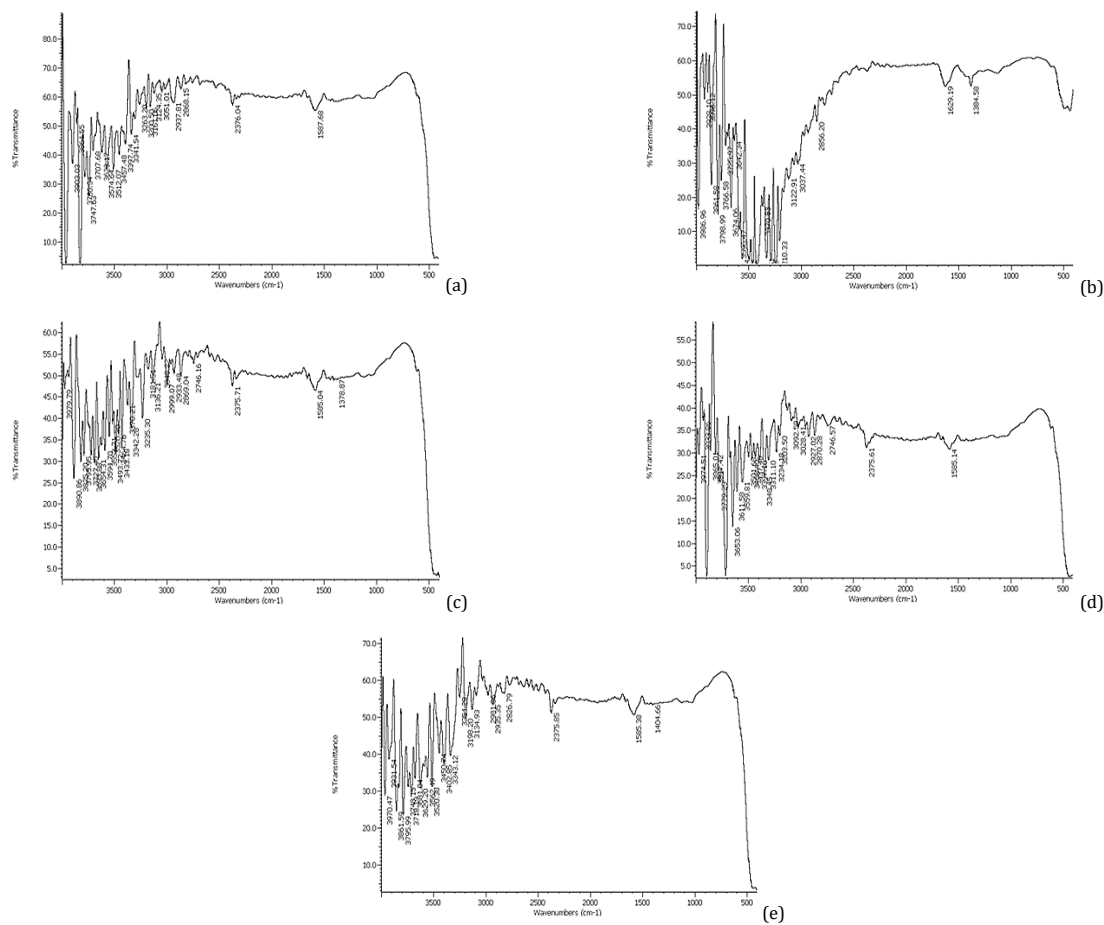


Figure 2. IR spectrum of (a) ZNB-1, (b) ZNB-2, (c) ZNB-3, (d) ZNB-4 and (e) ZNB-5.

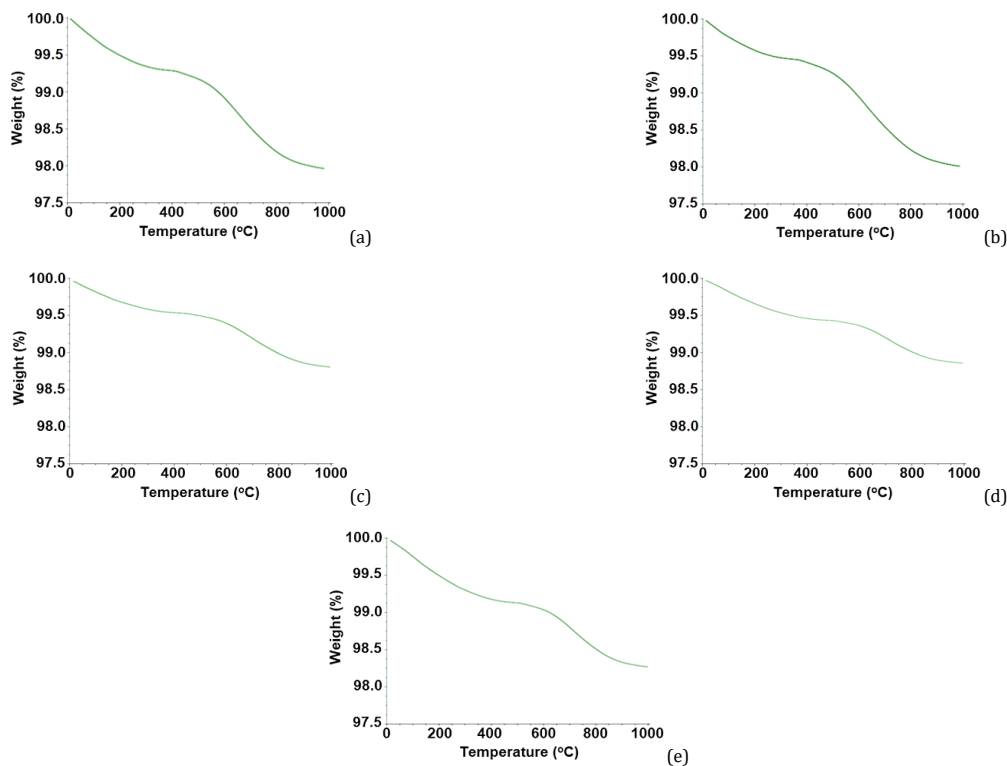


Figure 3. TGA curve of (a) ZNB-1, (b) ZNB-2, (c) ZNB-3, (d) ZNB-4 and (e) ZNB-5.

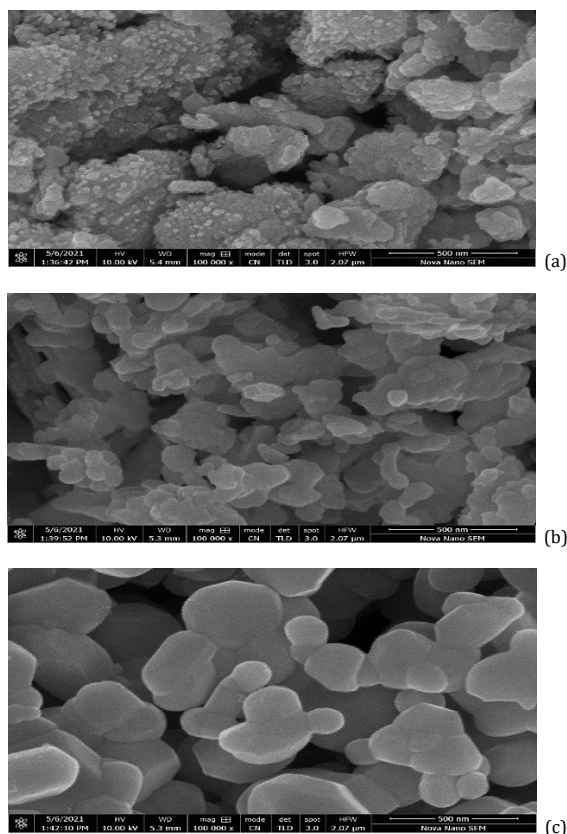


Figure 4. SEM micrograph of (a) ZNB-1, (b) ZNB-3, and (c) ZNB-5.

Former scientists also obtained highly agglomerated zinc oxide nanoparticles of various shapes that separated after calcination at higher temperatures and attained regular shapes [16,17,20].

#### 4. Conclusion

Zinc oxide nanoparticles were prepared through a cost-effective sol-gel method using a basic medium. The effect of varying calcination temperatures on the structure and morphology of the prepared samples were investigated. X-ray diffraction analysis confirmed that all the samples were composed of pure hexagonal wurtzite structure of zinc oxide. IR spectroscopy identified the presence of surface hydroxyl groups and organic residues entrapped in the nanocrystals while TGA proved their thermal stability. FESEM studies showed that calcination at 500 °C led to increased agglomeration followed by a significant decrease due to the separation of nanoparticles with the temperature rise. The particle size on the other hand increased due to particle growth at higher calcination temperatures resulting in the formation of nano-flakes.

#### Disclosure statement

Conflict of interest: The authors declare that they have no conflict of interest. Ethical approval: All ethical guidelines have been adhered. Sample availability: Samples of the compounds are available from the author.

#### CRedit authorship contribution statement

Conceptualization: Samreen Zahra; Methodology: Samreen Zahra; Validation: Samreen Zahra; Investigation: Saboora Qaisar; Resources: Hamim Bukhari; Data Curation: Asma Sheikh; Writing - Original Draft: Samreen Zahra; Writing-Review and Editing: Samreen Zahra; Visualization: Samreen Zahra;

Supervision: Chaudhry Athar Amin; Project Administration: Chaudhry Athar Amin.

#### ORCID and Email

Samreen Zahra

 [samreenzahra68@hotmail.com](mailto:samreenzahra68@hotmail.com)

 <https://orcid.org/0000-0001-5504-7816>

Saboora Qaisar

 [sabooraqaisar@gmail.com](mailto:sabooraqaisar@gmail.com)

 <https://orcid.org/0000-0002-4699-4616>

Asma Sheikh

 [asmashkhs@yahoo.com](mailto:asmashkhs@yahoo.com)

 <https://orcid.org/0000-0002-5632-785X>

Hamim Bukhari

 [a1hamim@yahoo.com](mailto:a1hamim@yahoo.com)

 <https://orcid.org/0000-0003-2887-452X>

Chaudhry Athar Amin

 [headmprc2021@gmail.com](mailto:headmprc2021@gmail.com)

 <https://orcid.org/0000-0002-4490-4357>

#### References

- [1]. Kołodziejczak-Radzimska, A.; Jesionowski, T. Zinc oxide-from synthesis to application: A review. *Materials (Basel)* **2014**, *7*, 2833–2881.
- [2]. Shaba, E. Y.; Jacob, J. O.; Tijani, J. O.; Suleiman, M. A. T. A critical review of synthesis parameters affecting the properties of zinc oxide nanoparticle and its application in wastewater treatment. *Appl. Water Sci.* **2021**, *11*, 48–89.
- [3]. Naveed Ul Haq, A.; Nadhman, A.; Ullah, I.; Mustafa, G.; Yasinzai, M.; Khan, I. Synthesis approaches of zinc oxide nanoparticles: The dilemma of ecotoxicity. *J. Nanomater.* **2017**, *2017*, 1–14.
- [4]. Fardood, S. T.; Ramazani, A.; Moradnia, F.; Afshari, Z.; Ganjkanlu, S.; Zare, F. Y. Green synthesis of ZnO nanoparticles via sol-gel method and investigation of its application in solvent-free synthesis of 12-aryl-

- tetrahydrobenzo[*a*]xanthene-11-one derivatives under microwave irradiation. *Chem. Methodol.* **2019**, *3*, 696–706.
- [5]. Davis, K.; Yarbrough, R.; Froeschle, M.; White, J.; Rathnayake, H. Band gap engineered zinc oxide nanostructures via a sol-gel synthesis of solvent driven shape-controlled crystal growth. *RSC Adv.* **2019**, *9*, 14638–14648.
- [6]. Verma, H. K.; Maurya, K. K. Synthesized zinc oxide nanomaterials studies of structural, optical and photocatalytic applications. *AIP Conference Proceedings* **2020**, *2220*, 140032.
- [7]. Konne, J. L.; Christopher, B. O. Sol-gel syntheses of zinc oxide and hydrogenated zinc oxide (ZnO:H) phases. *J. Nanotechnol.* **2017**, *2017*, 1–8.
- [8]. Arya, S.; Mahajan, P.; Mahajan, S.; Khosla, A.; Datt, R.; Gupta, V.; Young, S.-J.; Oruganti, S. K. Review—Influence of processing parameters to control morphology and optical properties of sol-gel synthesized ZnO nanoparticles. *ECS J. Solid State Sci. Technol.* **2021**, *10*, 023002–023023.
- [9]. Lu, X.; Kanamori, K.; Nakanishi, K. Preparation of zinc oxide with a three-dimensionally interconnected macroporous structure via a sol-gel method accompanied by phase separation. *New J Chem* **2019**, *43*, 11720–11726.
- [10]. Vishwakarma, A. Synthesis of zinc oxide nanoparticle by sol-gel method and study its characterization. *Int. J. Res. Appl. Sci. Eng. Technol.* **2020**, *8*, 1625–1627.
- [11]. Somoghi, R.; Purcar, V.; Alexandrescu, E.; Gifu, I. C.; Ninciuleanu, C. M.; Cotrut, C. M.; Oancea, F.; Stroescu, H. Synthesis of zinc oxide nanomaterials via sol-gel process with anti-corrosive effect for Cu, Al and Zn metallic substrates. *Coatings* **2021**, *11*, 444–458.
- [12]. Fakhari, S.; Jamzad, M.; Kabiri Fard, H. Green synthesis of zinc oxide nanoparticles: a comparison. *Green Chem. Lett. Rev.* **2019**, *12*, 19–24.
- [13]. Hasnidawani, J. N.; Azlina, H. N.; Norita, H.; Bonnia, N. N.; Ratim, S.; Ali, E. S. Synthesis of ZnO nanostructures using sol-gel method. *Procedia Chem.* **2016**, *19*, 211–216.
- [14]. Mehar, S.; Khoso, S.; Qin, W.; Anam, I.; Iqbal, A.; Iqbal, K. Green Synthesis of Zinc oxide Nanoparticles from Peganum harmala, and its biological potential against bacteria. *Front. nanosci. nanotechnol.* **2019**, *6*, 1–5.
- [15]. Narayana, A.; Bhat, S. A.; Fathima, A.; Lokesh, S. V.; Surya, S. G.; Yelamagad, C. V. Green and low-cost synthesis of zinc oxide nano particles and their application in transistor-based carbon monoxide sensing. *RSC Adv.* **2020**, *10*, 13532–13542.
- [16]. Thi Tran, Q. M.; Thi Nguyen, H. A.; Doan, V.-D.; Tran, Q.-H.; Nguyen, V. C. Biosynthesis of zinc oxide nanoparticles using aqueous Piper beetle leaf extract and its application in surgical sutures. *J. Nanomater.* **2021**, *2021*, 1–15.
- [17]. Singh, N.; Haque, F. Z. Synthesis of zinc oxide nanoparticles with different pH by aqueous solution growth technique. *Optik (Stuttg.)* **2016**, *127*, 174–177.
- [18]. Alamdari, S.; Sasani Ghamsari, M.; Lee, C.; Han, W.; Park, H.-H.; Tafreshi, M. J.; Afarideh, H.; Ara, M. H. M. Preparation and characterization of zinc oxide nanoparticles using leaf extract of *Sambucus ebulus*. *Appl. Sci. (Basel)* **2020**, *10*, 3620–3638.
- [19]. Bagabas, A.; Alshammari, A.; Aboud, M. F.; Kosslick, H. Room-temperature synthesis of zinc oxide nanoparticles in different media and their application in cyanide photodegradation. *Nanoscale Res. Lett.* **2013**, *8*, 516–525.
- [20]. Mei, L. F.; Liang, K. M. Crystallization behavior of Mg-doped Titania. *Key Eng. Mater.* **2010**, *434–435*, 847–849.
- [21]. Šćepanović, M.; Abramović, B.; Golubović, A.; Kler, S.; Grujić-Brojčin, M.; Dohčević-Mitrović, Z.; Babić, B.; Matović, B.; Popović, Z. V. Photocatalytic degradation of metoprolol in water suspension of TiO<sub>2</sub> nanopowders prepared using sol-gel route. *J. Solgel Sci. Technol.* **2012**, *61*, 390–402.
- [22]. Sharma, G.; Soni, R.; Jasuja, N. D. Phytoassisted synthesis of magnesium oxide nanoparticles with *Swertia chirayita*. *J. Taibah Univ. Sci.* **2017**, *11*, 471–477.
- [23]. Lopez-Iso, P.; Pugliese, D.; Boetti, N.; Janner, D.; Baldi, G.; Petit, L.; Milanese, D. Design, synthesis, and structure-property relationships of Er<sup>3+</sup>-doped TiO<sub>2</sub> luminescent particles synthesized by sol-gel. *Nanomaterials (Basel)* **2018**, *8*, 20–33.
- [24]. Ramimoghadam, D.; Bagheri, S.; Abd Hamid, S. B. Biotemplated synthesis of anatase titanium dioxide nanoparticles via lignocellulosic waste material. *Biomed Res. Int.* **2014**, *2014*, 205636.
- [25]. Wong, M.-S.; Chen, C.-W.; Hsieh, C.-C.; Hung, S.-C.; Sun, D.-S.; Chang, H.-H. Antibacterial property of Ag nanoparticle-impregnated N-doped titania films under visible light. *Sci. Rep.* **2015**, *5*, 11978–11988.
- [26]. Meshesha, D. S.; Matangi, R. C.; Tirukkavalluri, S. R.; Bojja, S. Synthesis and characterization of Ba<sup>2+</sup> and Zr<sup>4+</sup> co-doped titania nanomaterial which in turn used as an efficient photocatalyst for the degradation of rhodamine-B in visible light. *S. Afr. J. Chem. Eng.* **2017**, *23*, 10–16.
- [27]. Ahmad, S.; Saeed, A. Synthesis of metal/silica/Titania composites for the photocatalytic removal of methylene blue dye. *J. Chem.* **2019**, *2019*, 1–6.
- [28]. Trivedi, M. K.; Dahryn Trivedi, A. B. Spectroscopic characterization of disodium hydrogen orthophosphate and sodium nitrate after biofield treatment. *J. Chromatogr. Sep. Tech.* **2015**, *6* (5), 282–286.
- [29]. Arshad, M.; Qayyum, A.; Abbas, G.; Haider, R.; Iqbal, M.; Nazir, A. Influence of different solvents on portrayal and photocatalytic activity of tin-doped zinc oxide nanoparticles. *J. Mol. Liq.* **2018**, *260*, 272–278.
- [30]. Mahamuni, P. P.; Patil, P. M.; Dhanavade, M. J.; Badiger, M. V.; Shadija, P. G.; Lokhande, A. C.; Bohara, R. A. Synthesis and characterization of zinc oxide nanoparticles by using polyol chemistry for their antimicrobial and antibiofilm activity. *Biochem. Biophys. Rep.* **2019**, *17*, 71–80.
- [31]. Zaid, H. M.; Fakhruddin, H.; Yow, F. Y.; Razali, N.; Dasan, Y. K. Synthesis and characterization of titanium dioxide nanoparticles for application in enhanced oil recovery. *Defect Diffus. For.* **2019**, *391*, 74–81.
- [32]. Endres, S. C.; Ciacchi, L. C.; Mädler, L. A review of contact force models between nanoparticles in agglomerates, aggregates, and films. *J. Aerosol Sci.* **2021**, *153*, 105719–105757.
- [33]. Mohd Yusof, H.; Mohamad, R.; Zaidan, U. H.; Abdul Rahman, N. A. Microbial synthesis of zinc oxide nanoparticles and their potential application as an antimicrobial agent and a feed supplement in animal industry: a review. *J. Anim. Sci. Biotechnol.* **2019**, *10*, 57–78.



Copyright © 2022 by Authors. This work is published and licensed by Atlanta Publishing House LLC, Atlanta, GA, USA. The full terms of this license are available at <http://www.eurjchem.com/index.php/eurjchem/pages/view/terms> and incorporate the Creative Commons Attribution-Non Commercial (CC BY NC) (International, v4.0) License (<http://creativecommons.org/licenses/by-nc/4.0>). By accessing the work, you hereby accept the Terms. This is an open access article distributed under the terms and conditions of the CC BY NC License, which permits unrestricted non-commercial use, distribution, and reproduction in any medium, provided the original work is properly cited without any further permission from Atlanta Publishing House LLC (European Journal of Chemistry). No use, distribution or reproduction is permitted which does not comply with these terms. Permissions for commercial use of this work beyond the scope of the License (<http://www.eurjchem.com/index.php/eurjchem/pages/view/terms>) are administered by Atlanta Publishing House LLC (European Journal of Chemistry).